

Recovery of lead from copper anode slime and study of kinetics of lead dissolution

Sattar Ghader^{1*}, Hamed Rezaei¹ & Abbas Ghareghashi^{2*}

Department of Chemical Engineering, College of Engineering, Shahid Bahonar University of Kerman, Kerman, Iran

Department of Chemical Engineering, Engineering Faculty, Velayat University, Iranshahr, Iran

*E-mail: a.ghareghashi@velayat.ac.ir (AG), sattarghader@yahoo.com / ghader@uk.ac.ir (SG)

Received 2 August 2023; accepted 4 January 2024

In this study, an effective method of recovering metallic lead from copper anode slime is investigated. A method of leaching with nitric acid at atmospheric pressure is also proposed, and the effect of various factors on the leaching effect is studied. The kinetics of leaching is studied, and a model of the leaching process is established. Copper anode slime residues, rich in valuable metals, provide one of the critical resources for recycling metals in favourable conditions. A green acid leaching process for lead (Pb) enrichment from copper (Cu) anode slime is developed in this study. Under ideal conditions, HNO₃ successfully leached 72% Pb in 2 h. The optimum leaching conditions are the stirring speed of 1000 rpm, the temperature of 90 °C, the HNO₃ concentration of 4 M, and the solution-to-anode slime ratio of 10:1. The kinetics of lead leaching from anode slime is developed according to the phase composition and shape of the leaching residue and raw material. The modified grain model is considered for this purpose. MATLAB is used to solve the model in isothermal mode by using the orthogonal collocation method. The results are good compatibility with experimental data. The activation energy is calculated using the parameters derived from the modified tablet-grain model based on the test conditions. Therefore, the lead recovery under the proposed process has a promising potential for treating Cu anode slime.

Keywords: Acid leaching, Copper anode slime, Leaching kinetic, Lead extraction, Lead recovery

Introduction

The need of metals in the industries has led to the discovery and extraction of these materials. Lead (Pb) is one of the incredibly useful metals in the industry as well as one of the main pollutants in the environment¹. It is found in the earth's crust in small quantities. In the past, it was used for glazing dishes, pharmaceuticals, and water transport means, which were later banned due to their poisoning effects.

There are some restrictions and use of Pb streams in a way to meet the environmental standards for Pb^(Ref. 2). The use of this metal for various applications includes Pb sheets, cable covers, ammunition, pesticides, etc. A substantial proportion of the world's Pb production is produced from direct processing of the most commonly found ore lead sulfide (PbS). However, recovering this valuable metal from copper anode slime can be also considered an additional supply source for it³⁻⁷. During copper electro refining, anode slime is accumulated underneath copper electrolysis cells, which contains some amounts of copper, lead, silver, and selenium, as well as very less amount of gold.

The recovery of valuable metals (e.g., silver, gold, and lead) from anode slime has attracted the

researcher's attention to put it to practical use⁸⁻¹⁰. In order to improve the efficiency of leaching, anode slime needs to be pretreated with procedures that vary depending on the composition of the anode slime. These treatments aim to recover metals from anode slime by different methods, among which solvent leaching is the most convenient one. Depending on the composition of the leaching solution, various methods, such as ion exchange, electrowinning, precipitation, and solvent extraction can be utilized to separate metals from the solution to obtain the desired product^{10,11}.

Tokkan et al.^{12,13} used triethanolamine (TEA) to study Pb leaching from anode slime. In their study, important factors were reaction temperature, TEA concentration, leaching time, and solid/liquid ratio. The optimal process condition was 3.5 M TEA, 1/10 solid/liquid ratio, and 150 min of leaching time at 313 K. Liu et al.¹⁴ performed pretreatment of copper anode slime using alkaline pressure oxidative leaching followed by sulfuric acid leaching. The optimum conditions were a stirring speed of 750 rpm, an oxygen partial pressure of 0.7 MPa, temperature of 200 °C, leaching time of 3 h, solid-to-liquid ratio of 1:5, and 2.0 mol/L NaOH. The leaching ratio for Pb

was only 3.0%. The X-ray diffraction (XRD) analysis showed that the phase of lead sulfate in copper anode slime was transformed into lead hydroxide.

Li et al.¹⁵ studied separation of metals from copper anode slime by alkali-fusion-leaching. The slime was fused with NaNO_3 and NaOH , followed by water leaching. About 76% of Pb was leached under optimal conditions, while only 3.5% of Sb (antimony) and 1.5% of Cu were dissolved. Cu, Sb, Pb, and Ag in the residue were present as CuO , NaSb(OH)_6 , PbO , and Ag, respectively. NaOH /slime mass ratio of 2, slime/water mass ratio of 60, NaNO_3 /slime mass ratio of 0.33, leaching temperature of 60 °C, fusion temperature of 600 °C, fusion times of 45 min, and leaching times of 30 min were the optimum operating conditions. As the NaOH addition controlled the OH^- concentration of the leaching solution, it could significantly affect the extraction of Pb. A higher slime/water ratio increased the concentration of metals in leach liquor, nonetheless at a lower recovery of Pb extraction. NaNO_3 addition caused enrichment of metals in residue and in solution. Rüşen and Topçu¹⁶ looked into how an acidic ionic liquid, 1-ethyl-3-methyl-imidazolium hydrogen sulfate, could be used to get gold out of copper anode slime. Their leaching experiments showed that 89% of gold can be recovered at the following conditions: 80% IL concentration, 75 °C, 4 h leaching time, and 1/25 g/mL solid/liquid ratio, while Pb, Se, Sn, and Te of anode slime had low dissolution in the ionic liquid. Zárate-Gutiérrez et al.¹⁷, studied Pb leaching from Pb-Ag-Zn concentrate in citrate solutions by hydrogen peroxide (H_2O_2). Complete Pb dissolution was achieved in 90 min, and the initial kinetics became faster as the concentration of H_2O_2 increased (due to the higher solution potential). A very small amount of impurities (Ag, Zn) were dissolved and remained in the residues. Khaleghi et al.¹⁸ studied silver recovery from copper anode slime. They aimed to synthesize silver nanoparticles from a secondary source that contains silver as well as some other metals. They experimentally determined the optimum condition for silver leaching from copper anode slime in a nitric acid solution, followed by the removal of other metals from the anode slime that may co-precipitate with silver during the nanoparticle synthesis experiment. In addition, experimental variables were also studied in detail to find their effect on the size of silver nanoparticles. The kinetics study was the main interest of their study.

Dong et al.¹⁹ studied lead, selenium, gold, copper, and silver recovery from copper anode slime by an economical hydrometallurgical method. In their method, a lead concentrate with a lead grade of 57.2% was obtained after removing selenium, copper, gold, and silver from anode slime. The economic analysis showed an income of 702217.8 CNY for treating one ton of anode slime, confirming the good potential of the proposed method. In another study, Palden et al.²⁰ used ethylenediaminetetraacetic acid (EDTA) for lead removal from soil owing to its high lead extraction efficiency and the high thermodynamic stability of the $\text{Pb(II)}\text{-EDTA}$ complex. Almost 72-80% lead recovery was obtained in the first leaching time of 1 h at room temperature using 0.05 mol/L EDTA after optimizing the EDTA concentration, liquid-to-solid ratio, temperature, pH, and leaching time. The main advantage was the high selectivity towards lead with a minimum co-dissolution of iron, which reduced chemical consumption and simplified downstream processes. 100% leaching of lead could be obtained via multi-step leaching, where the leaching residues were contacted by a fresh EDTA solution three times²⁰.

Gargul et al.²¹ studied leaching of Pb flash-smelting slag with citric acid. The parameters were optimized so that the Pb content in the post-leaching sediment was 0.41-0.6% while it was 3% in flash-smelting slag. The leaching was continued in the second step using sulfuric acid solutions, and almost 100% lead recovery was obtained.

Acid leaching of Pb has been considered an alternative to high-temperature processes because it offers improved energy consumption and production costs, increased selectivity, and a lead recovery rate from slime. In previous research, various solutions such as citric acid²², phosphate fertilizers²³, calcium chloride²⁴, and ferric sulfate and sulfuric acid²⁵ were used for the recovery of lead. This paper involves the recovery of lead from copper anode slime. The leaching process was performed with nitric acid at atmospheric pressure. The effects of the main parameters were explored, and a kinetic model was revealed to describe the proposed leaching process.

Experimental Section

The used chemicals were of reagent grade. The copper anode slimes were prepared at the Sarcheshmeh copper complex in Iran. The slime was crushed in a lab-scale mill. Mineralogy, the

morphology of slime, and element analysis were conducted by X-ray fluorescence (XRF), XRD, and scanning electron microscopy (SEM), respectively. The atomic absorption (AAS), XRF, XRD, and SEM spectroscopy equipment's models were Varian (Australia), ARL 8410, ARL 8410, and Phillips, respectively.

Experiments were performed at atmospheric pressure. In each experiment, 30 g of slime was added to 300 mL of nitric acid solution, which was rigorously mixed. The solid-to-solution ratio was 1:10. A magnetic stirrer was used to completely agitate the solution at 1000 rpm on the hotplate. When the solution temperature reached the desired amount, 30 g of anodic slime was added. A lid was used on the vessel entrance to prevent the solution from evaporating too much. The experiments were conducted at 25, 40, 60, and 90 °C and nitric acid concentrations of 0.1, 0.5, 1, 2, and 4 M for 2 h.

At different time steps (1, 3, 5, 10, 20, 30, 40, 50, 60, 90, and 120 min), 5 mL of leaching solution was filtered by filter paper and was sampled from the solution. Since high concentrations of lead cannot be measured by AAS, the sample should be diluted in the range of 1-10 ppm. 1 mL of the filtered sample was taken with a sampler and diluted in a 500 mL volumetric flask with distilled water. AAS analyzed the diluted solution to determine the percentage of lead in the sample. The stirrer speed was adjusted to 1000 rpm to eliminate the mixing effect and ensure complete mixing in the leaching solution. The brown NO vapour with a reddish tint was detected over the nitric acid leaching solution at the start of the process. Therefore, percentage of lead recovery was calculated as follow:

$$\% \text{ Recovery} = \left(\frac{a}{b}\right) \times 100 \quad \dots(1)$$

Where, a and b are mass of Pb in the leaching solution and in initial solid anode slime, respectively. To calculate the mass of Pb in the leaching solution, the concentration of the sample taken from the solution was measured and multiplied by the volume of the sample. However, the cost of the sample volume was not taken into account.

Results and Discussion

Analysis of anode slime

The chemical analysis of the sample consisting of the anode slime using XRF showed that in the anode slime, there was 5.7 wt% lead (Table 1). Fig. 1 shows the XRD pattern of the anode slime sample. As shown

in this figure, the main phases of slime are Cu_9S_5 , PbSO_4 , Cu_4Te_3 , and Fe. It also shows that one of the main phases of slime is anglesite (PbSO_4). Approximately uniform dispersion of the fine and large particles can be observed from the SEM image of anode slime shown in Fig. 2. Some spherical clusters and a small amount of fine particles are observed. The quantitative values of the chemical results of the main components of anode slime are given in Fig. 3. It shows Pb, Se, Cu, Sb, and Ag are major components of anode slime.

Determination of the highest lead recovery conditions

The leaching of copper anode slime performed at atmospheric pressure using nitric acid as it has very high oxidizing power. Use of nitric acid is preferred over sulfuric acid as with the latter an insoluble compound lead sulfate was precipitated out. So, to dissolve the amount of lead present in the sludge in the acid i.e., for the leaching operation, temperature and concentration of the acid have to be increased. For example, to perform the leaching operation with sulfuric acid, the temperature should be 90 °C and the concentration of the acid should be 16 M so that some lead was dissolved in about 20%, but with nitric acid at the same temperature and lower concentration of nitric acid, a very large percentage of lead was

Table 1 — Anode slime chemical composition observed by XRF

Component	Percentage (%)	Component	Percentage (%)
Se	15.35	Ti	0.059
Ba	30.37	Ag	12.29
Fe	1.04	Sb	3.92
Sr	0.12	Pb	5.30
As	2.07	SiO_2	2.98
Mg	0.15	Cu	5.65
Te	0.95	Sr	1.18
S	16.91	Sn	0.35
Sr	1.18	Au	0.019
K	0.11	L. O. I	0.0

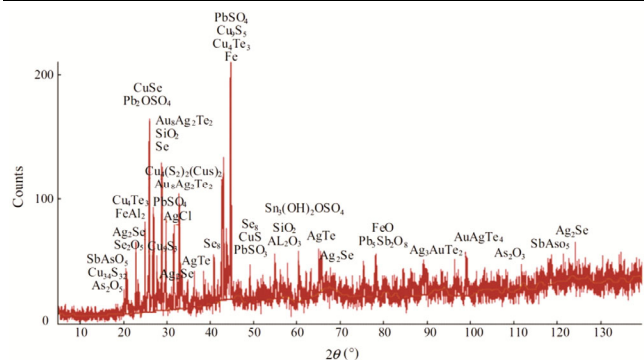


Fig. 1 — XRD pattern of copper anode slime

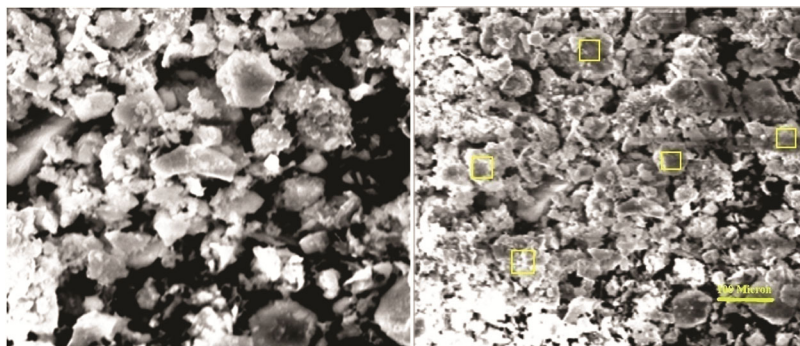


Fig. 2 — SEM images (at different magnifications) of copper anode slime

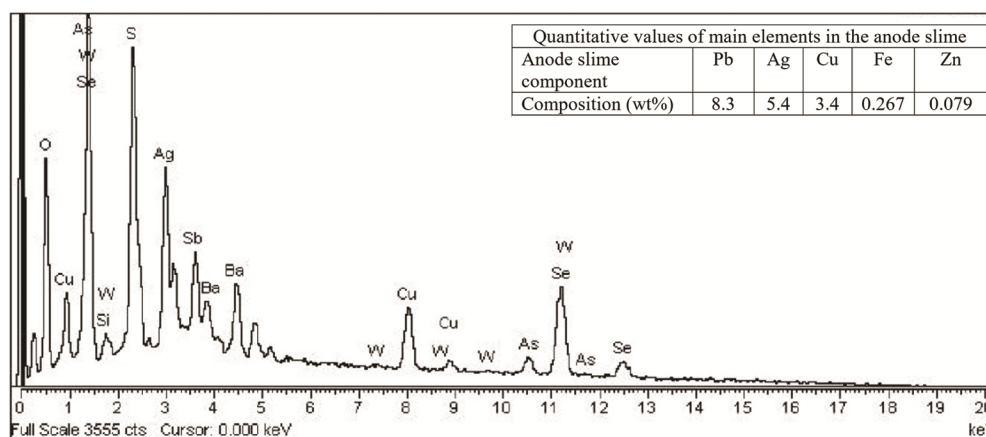


Fig. 3 — EDS analysis of copper anode slime

dissolved. Experiments were performed under various conditions (i.e., different solution temperatures, leaching times, and acid concentrations). Finally, concentration of lead was measured in the solution. The temperature and acid concentration domains are presented in Table 2. At the beginning of the leaching process, lead concentration gradually increased in the solution due to lead removal from anode slime. Fig. 4 shows lead recovery at different temperatures and nitric acid concentrations. The lead recovery increased by increasing the nitric acid concentration from 0.1 to 4.0 M, while it hardly increased with the concentration increasing from 2.0 to 4.0 M. In general, the rise in the concentration of nitric acid is what causes the amount of nitric acid per unit volume to rise. This is because copper reacts with more nitric acid in the same amount of anode slime. 90 °C leaching temperature effectively enhanced lead recovery due to the effective collision of molecules. Notably, the temperature increase softly results in lead elimination from the anode slime. Approximately 90% of lead was recovered up to 40 min; after this, lead recovery remained approximately unchanged (Fig. 4). Using a nitric acid concentration of 4.0 M at

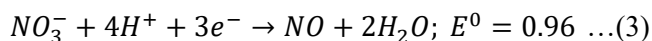
Table 2 — Domains of nitric acid concentration and the leaching temperature used in experiments

Parameter	Value
Concentration of nitric acid (M)	0.1, 0.5, 1, 2, 4
Temperature of experiments (°C)	25, 40, 60, 90

90 °C led to 71% lead recovery, indicating the best conditions for lead recovery from anode slime.

Effect of temperature and acid concentration

Fig. 5 shows the variations of lead recovery vs. nitric acid concentration. Lead is effectively removed at nitric acid concentrations above 4 M (71%). In the leaching solution, the lead dissolution was due to the high ability of nitric acid to oxidize. The nitric acid reaction in a dilute solution is as follows:



During the tests in the nitric acid solution, a reddish-brown vapour was created, which was NO. Eq. (4) shows the difference in the reduction potentials of the two half-cells in a diluted solution

$$\Delta E = 0.0591/(n \log K) \dots(4)$$

where F, n, and K denote the Faraday constant, electron number, and reaction equilibrium expression,

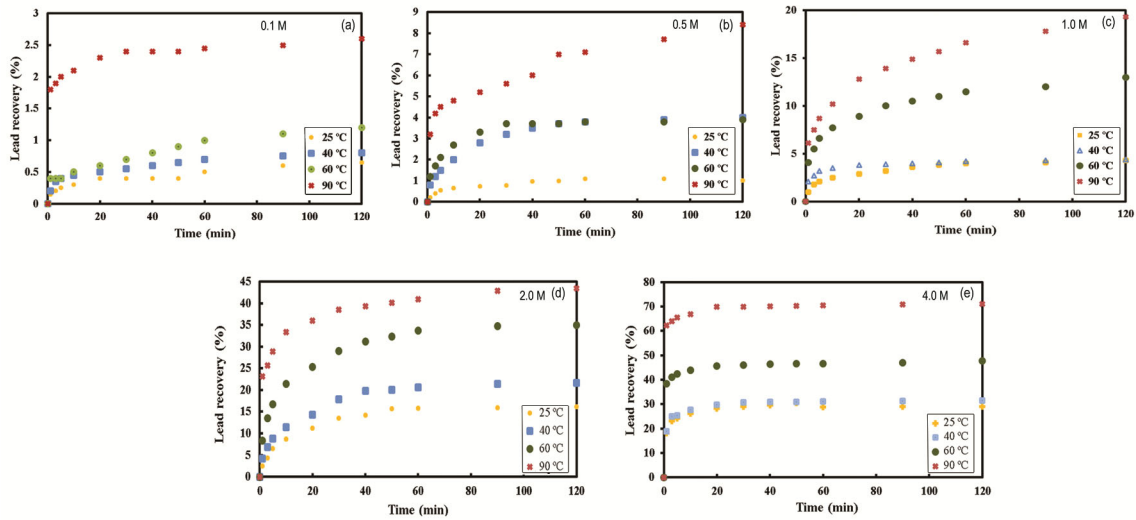


Fig. 4 — Lead recovery at different temperatures and nitric acid concentrations

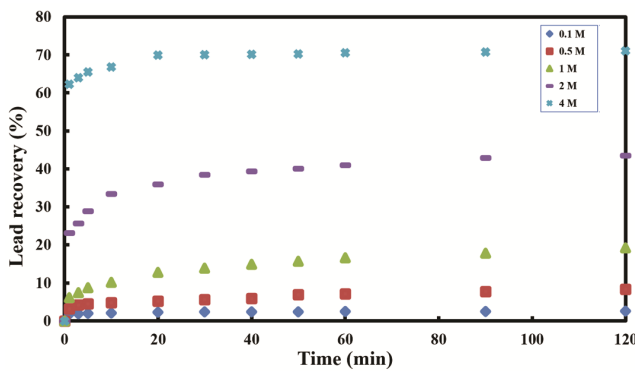


Fig. 5 — Plot for the influence of nitric acid concentrations on lead recovery from copper anode slime at 90 °C

respectively. Moreover, the Nernst equation is used for estimating the half-reaction potential (E) of nitric acid as follows:

$$E = E^0 + 0.0591 / (3 \log[(H^+)^4(NO_3^-)/(P_{NO})]) \dots (5)$$

where, R , $(H^+)^4$, (NO_3^-) , and (P_{NO}) denote universal gas constant and concentrations of $(H^+)^4$, (NO_3^-) , and (P_{NO}) , respectively. According to Eq. (4), nitric acid at 4 M had higher lead recovery than lower molarities. This equation predicts an increase in the reduction potential (increase in oxidizing ability) as the acidity and molarity of nitric acid increase. With increasing oxidizing ability, nitric acid would solubilize more lead. These predictions have been confirmed experimentally.

Effect of leaching time

There was a significant effect of time on leaching for lead recovery (Fig. 6). In the starting of the leaching process, more lead was solubilised in nitric

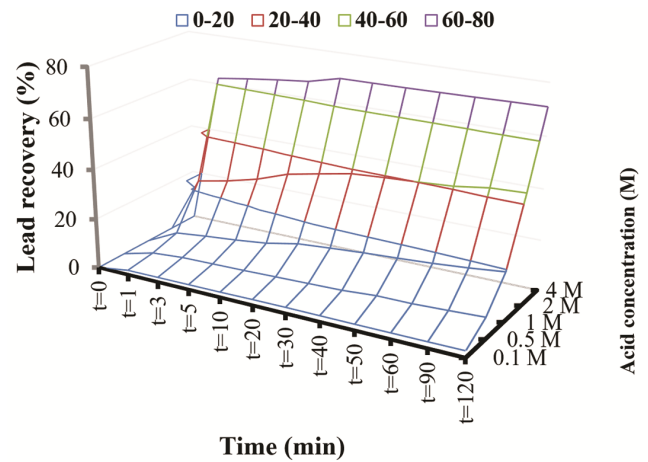


Fig. 6 — Three-dimensional profiles of lead recovery from copper anode slime in terms of leaching time and nitric acid concentrations at temperature 90 °C

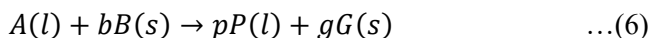
acid. After some time i.e., 120 min, lead recovery did not changed further, showing that this layer was not dissolved more in nitric acid. Film-forming occurred because of the slowdown of leaching at the end of the process. For the surface layer, increasing the thickness reduced the acid diffusion to the anode slim particles' surface.

Leaching kinetic

Understanding the mechanism of a leaching system is the main consideration. There are numerous applications of systems containing heterogeneous fluid-solid reactions for hydrometallurgical and chemical processes. In general, it is possible to control the reaction rate of liquid-solid systems by one of the following steps: chemical reaction on the core surface of unreacted material, diffusion through

ash, or the fluid film²⁶. The modified particle-pellet model was used to specify the rate-controlling step and kinetic parameters²⁷. The assumption made in this model is that the solid structure consists of several smaller particles or grains. The reactant gas penetrates between the grains and reacts on their surface. The reaction takes place on the surface of each grain, according to the supply chain management model. As a result, a solid product layer is formed around each grain, creating a penetration resistance for the gas to penetrate the tablet²⁶. The particle-pellet model is modified by considering the effect of the reaction on its structure. By penetrating the gaseous reactant into the particle, the reaction takes place on the particle's surface. Because of the difference between the molar volumes of the reactive solid and the product solid, the change occurs in the solid structure²⁸. A schematic of the modified grain model is shown in Fig. 7.

This reaction model among a fluid and a solid can be represented as Eq. (6).



where, B is a solid reactant and as the reaction progresses, a layer of solid product forms around the unreacted core. Due to the stoichiometric coefficient difference and the difference between the molar volume of the solid reactant and the layer of solid product, the particles' radius changes²⁷.

The following assumptions were considered regarding this model:

1. The grain's shape is spherical and its shape and size are constant during the reaction.
2. Pseudo-steady state and isothermal approximations are valid.
3. Effective gaseous diffusivity does not change during the course of the reaction.
4. The solid product around each grain is highly porous. Thus, the resistance of this product layer is negligible.

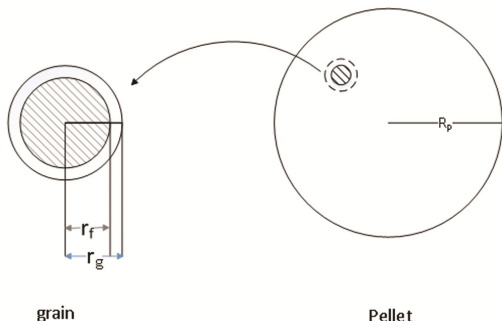


Fig. 7 — Schematic of modified grain model

5. Diffusion within the pellet is an equimolar counter-diffusion.
6. The solid structure is unaffected by the reaction.
7. Porosity and intergrain diffusion vary with the progress of the reaction.

From the mass balance, the dimensionless equation of gas penetration into the disk is as follows²⁹:

$$\frac{1}{\xi^2} \frac{\partial}{\partial \xi} \left(\delta \xi^2 \frac{\partial \alpha}{\partial \xi} \right) = \frac{\alpha r^{*2} \sigma^2}{1+6(r^* - (r^{*2}/r^{**}))\sigma_g^2} \quad \dots(7)$$

$$\frac{\partial r^*}{\partial \theta} = - \frac{\alpha r^{*2} \sigma^2}{1+6(r^* - (r^{*2}/r^{**}))\sigma_g^2} \quad \dots(8)$$

where, $\xi = \frac{r}{R}$ is dimensionless penetration distance inside the pellet, $\theta = v_b k_s c_{Ag} M_B t / \rho_B r_{g_0}$ is dimensionless time, $\alpha = \frac{C_A}{C_{Ag}}$ is the dimensionless

concentration of gaseous pellet reactants, $r^* = r_{g_c} / r_{g_0}$ is the dimensionless radius of the unreacted core in the particle, $r^{**} = r_g / r_{g_0}$ is the dimensionless particle radius, r_g is particle radius at time t, r_{g_0} is particle initial radius, and r_{g_c} is the unreacted core radius in the particle. The boundary and initial conditions are as follows:

$$\theta = 0, r^* = 1 \quad \dots(9)$$

$$\xi = 0, \frac{\partial \alpha}{\partial \xi} = 1 \quad \dots(10)$$

$$\xi = 1, \alpha = 1 \quad \dots(11)$$

r^{**} in Eqs. (6) and (7) is calculated using Eq. (12).

$$r^{**} = [Z_v + (1 - Z_v)r^{*3}]^{1/3} \quad \dots(12)$$

where, Z_v equation is calculated by Eq. (13)³⁰.

$$Z_v = \frac{g \rho_B M_g}{b \rho_g M_B (1 - \varepsilon_g)} \quad \dots(13)$$

where, ε_g and ε are product layer porosity and pellet porosity. As they are time- and place-dependent parameters, they can follow Eq. (14)³¹.

$$\frac{1 - \varepsilon}{1 - \varepsilon_0} = r^{**3} \quad \dots(14)$$

Porosity can also be related to Z_v using Eqs.(12) and (14) as follow:

$$\frac{\varepsilon}{\varepsilon_0} = 1 - \left(\frac{1 - \varepsilon}{\varepsilon_0} \right) [(Z_v - 1)(1 - r^{*3})] \quad \dots(15)$$

The diffusion coefficient is generally a function of solid porosity. Assuming that the cavities of the solid particle are large enough, the Knudson diffusion coefficient is not limiting, and the effective diffusion coefficient (D_e) is calculated using Eq. (16)³².

$$D_e = \frac{\varepsilon}{\tau_t} D_m \quad \dots(16)$$

where, τ_t , ε , and D_m are modulus of torsion, bed porosity and molecular diffusion coefficient, respectively. The solid nature and the porous solid structure affect these parameters. The function of the diffusion coefficient with the environment porosity and the method of changing the torsion coefficient in heterogeneous environments depends on the changes in the porous medium during the reaction, such as the growth and integration of cavities, the destruction or creation of new cavities or the closure of cavities and the formation of closed cavities, which in turn depends on the formed solid structure. These parameters change as the reaction progresses. By estimating the initial value of the effective diffusion coefficient (D_{e0}), it is possible to estimate the diffusion coefficient at all conversion percentages. The diffusion coefficient is obtained as follows³³.

$$D_e = \left(\frac{\varepsilon}{\varepsilon_0}\right)^\alpha D_{e0} \quad \dots(17)$$

In this equation, α is an experimental coefficient whose value is one according to the model of the single cavity model obtained by Ramachandran and Smith³⁴. According to the model of accidental cavities obtained by Wakao and Smith³⁵, this value is two. Considering this value based on the accidental cavities model, D_e is calculated using Eq. (18).

$$D_e = \left(\frac{\varepsilon}{\varepsilon_0}\right)^2 D_{e0} \quad \dots(18)$$

By placing D_e in Eq. (14), $\frac{D_e}{D_{e0}}$ is calculated as Eq. (18).

$$\frac{D_e}{D_{e0}} = \left(\frac{\varepsilon}{\varepsilon_0}\right)^2 = \left[1 - \left(\frac{1-\varepsilon}{\varepsilon_0}\right) [(Z_v - 1)(1 - r^{*3})]\right]^2 \quad \dots(19)$$

The primary slime porosity is one of the essential and effective parameters in the modified particle-pellet model. The quantitative and qualitative values must be specified first for process modelling. The porosity of anodic slime is very low. The BET test (Fig. 8) shows that the surface area of anode pores was 16.664 m²/g. This surface area was very small compared to the pore surface of the synthesized porous material. Therefore, the primary slime porosity amount should be considered low in the modified particle-pellet model.

Comparison of modified particle-pellet model with proposed model

A series of algebraic equations were created after modelling. The orthogonal collocation method was used as the best method to solve these equations.

The model results were compared with Prasannan's²⁸ work for the verification of the proposed model. A good agreement was obtained as shown in Fig. 9.

Modelling of experimental results

After ensuring the correctness of the equations, the experimental results obtained from different concentrations of nitric acid as well as leaching temperatures (1 M and 40 °C, 2 M and 60 °C, and 4 M and 90 °C) were compared with the results from the modified particle-pellet model (Figs. 10 (a-c)). In each condition, the parameters obtained from the model are reported in Table 3. As can be seen, the highest error between the model results and the laboratory data was observed at a concentration of 1 M and a temperature of 30 °C, but with the increase in concentration and temperature, this percentage of error reached less than 1%. It seems that lead cannot be removed efficiently from slime at 40 °C, and their reaction with acids at these temperatures is low, which becomes much more intense at higher temperatures (60 and 90 °C).

Determination of the reaction rate constant

The activation energy was calculated using Eq. (20) and laboratory results.

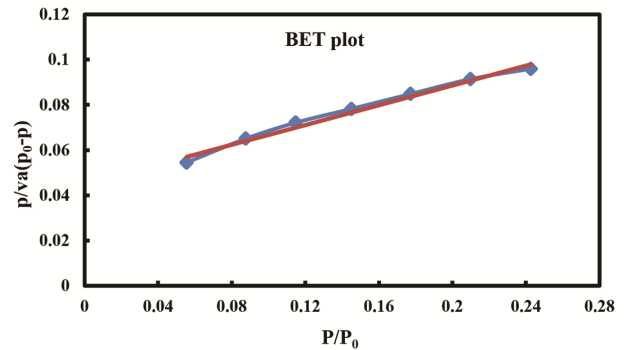


Fig. 8 — BET plot for determination of the solid surface

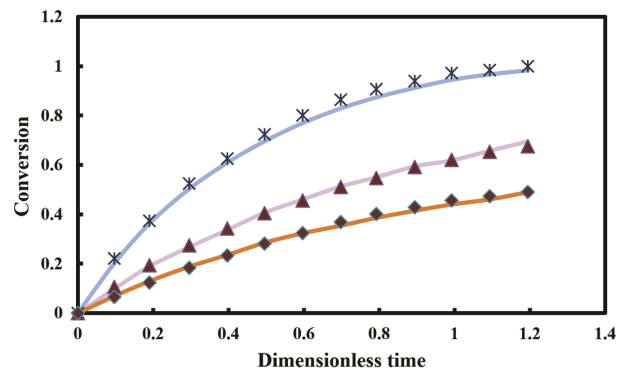


Fig. 9 — Comparison of model results with Prasannan work at $\sigma = 2, 6.3, 10, z = 1.5, \varepsilon = 0.5, \sigma_g^2 = 0.167$

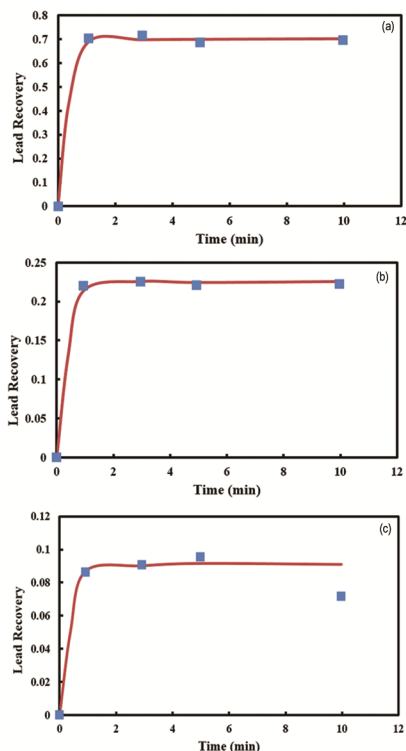


Fig. 10 — Comparison of the model and laboratory results using (a) 1 M acid and a temperature of 90 °C, (b) 2 M acid and a temperature of 60 °C, (c) 1 M acid and a temperature of 40 °C

Table 3 — The parameters obtained from the modified particle-pellet model

Condition	ε_0	σ	σ_g^2	z	$1/\tau$	Error (%)
1 M and 40°C	0.01	1	1.9	1.093	0.05	16.2
2 M and 60°C	0.01	1.2	0.9	1.0135	0.14	0.47
4 M and 90°C	0.01	1	1	1.0135	0.7	0.76

$$\frac{1}{\tau} = \frac{\vartheta_B \cdot k \cdot C_{Ag} \cdot M_B}{\rho_B r g_0} \quad \dots(20)$$

where, $\vartheta_B \cdot k \cdot C_{Ag} \cdot M_B$, and ρ_B are solid reactant kinematic viscosity, reaction rate constant, molar concentration of fluid, solid molecular weight and solid reactant density, respectively. The reaction rate constant was calculated using Eq. (21).

$$k = k_0 \exp\left(-\frac{E}{RT}\right) \rightarrow \ln k = \ln k_0 - \frac{E}{RT} \quad \dots(21)$$

where, E and k_0 are activation energy and pre-exponential factors, respectively. The reaction rate constant depends on $\frac{1}{\tau}$ and C_{Ag} while other parameters are constant. Activation energy can be obtained by fitting data based on Eq. (21). Fitting the data in Table 5 based on Eq. (20) is shown in Fig. 11.

Based on the data fitting, Eq. (21) is converted as follows:

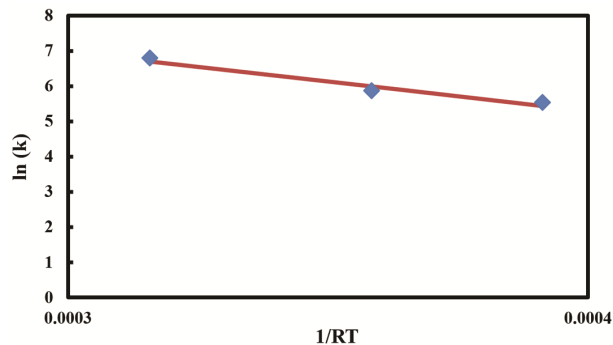


Fig. 11 — Data fitting of table 5 based on Eq. (19)

$$\ln(k) = 14.67 - \frac{199.78}{RT} \quad \dots(22)$$

The obtained activation energy value 199.78 kJ mol⁻¹ indicates a diffusion-controlled reaction.

Conclusion

This study investigated extracting lead from anode slime by leaching. The influence of various parameters, such as temperature, nitric acid concentration, and leaching time, on lead extraction from anode slime was studied to determine the optimal conditions for this process. The achieved results indicated that the optimum conditions for lead leaching were a solid/liquid ratio of 1:10 g/mL, a temperature of 90 °C, and a nitric acid concentration of 4 M. In optimum conditions, 71% of the lead was extracted from the copper anode slime. The results indicated that nitric acid concentration played a significant role in lead leaching. Moreover, the kinetic model of lead leaching from anode slime was developed based on the particle-pellet model. The model results were entirely verified with the Parsannan work. The high reaction rate resulted from the high activation energy of 199.78 kJ mol⁻¹.

References

- 1 Tiwari S, Tripathi I P & Tiwari H L, Lead poisoning -A review, *Res J Chem Sci*, 3 (2013) 86.
- 2 Cheng H & Hu Y, Lead (Pb) Isotopic fingerprinting and its applications in lead pollution studies in China: A review, *Environ Pollut*, 158 (2010) 1134.
- 3 Tishchenko A A, Extraction of selenium and tellurium from copper electrolytic slimes, *Chem Abstr*, 61 (1964) 3955.
- 4 Scott J D, Electrometallurgy of copper refinery anode slimes, *Metall Trans B*, 21 (1990) 629.
- 5 Nisar J, Ali G, Shah A, Shah M R, Iqbal M, Ashiq M N & Bhatti H N, Pyrolysis of expanded waste polystyrene: influence of nickel-doped copper oxide on kinetics, *Energy Fuel*, 33 (2019) 12666.
- 6 Naz S S, Islam N U, Shah M R, Alam S S, Iqbal Z, Bertino M, Franzel L & Ahmed A, Enhanced biocidal activity of

- Au nanoparticles synthesized in one pot using 2, 4-dihydroxybenzene carbodithioic acid as a reducing and stabilizing agent, *J Nanobiotechnol*, 11 (2013) 1.
- 7 Kanwal T, Kawish M, Maharjan R, Ghaffar I, Ali H S, Imran M, Perveen S, Saifullah S, Simjee S U & Shah M R, Design and development of permeation enhancer containing self-nanoemulsifying drug delivery system (SNEDDS) for ceftriaxone sodium improved oral pharmacokinetics, *J Mol Liq*, 289 (2019) 111098.
 - 8 Melo E, Hernández M C, Benavente O & Quezada V, Selenium dissolution from decopperized anode slimes in ClO⁻/OH⁻ Media, *Minerals*, 12 (2022) 1228.
 - 9 Rüşen A & Topçu M A, Investigation of an alternative chemical agent to recover valuable metals from anode slime, *Chem Pap*, 72 (2018) 2879.
 - 10 Moosavi-Khoonsari E, Mostaghel S, Siegmund A & Cloutier J P, A review on pyrometallurgical extraction of antimony from primary resources: Current practices and evolving processes, *Processes*, 10 (2022) 1590.
 - 11 Xing W D, Sohn S H & Lee M S, A Review on the recovery of noble metals from anode slimes, *Miner Process Extr Metall Rev*, 41 (2019) 130.
 - 12 Tokkan D & Donmez B, Optimal Analysis for leaching of lead from processed anode slime, *Acta Montan Slovaca*, 27 (2022) 40.
 - 13 Tokkan D, Çalban T, Kuşlu S, Çolak S & Dönmez B, Optimization of microwave-assisted removal of lead from anode slime in triethanolamine solutions, *Ind Eng Chem Res*, 51 (2012) 3903.
 - 14 Liu W, Yang T, Zhang D, Chen L & Liu Y, Pretreatment of copper anode slime with alkaline pressure oxidative leaching, *Int J Miner Process*, 128 (2014) 48.
 - 15 Li D, Guo X, Xu Z, Tian Q & Feng Q, Leaching behavior of metals from copper anode slime using an alkali fusion-leaching process, *Hydrometallurgy*, 157 (2015) 9.
 - 16 Rüşen A & Topçu M A, Optimization of gold recovery from copper anode slime by acidic ionic liquid, *Korean J Chem Eng*, 34 (2017) 2958.
 - 17 Zárate-Gutiérrez R, Gregorio-Vázquez L & Lapidus G T, Selective leaching of lead from a lead-silver-zinc concentrate with hydrogen peroxide in citrate solutions, *Can Metall Q*, 54 (2016) 305.
 - 18 Khaleghi A, Ghader S & Afzali D, Ag recovery from copper anode slime by acid leaching at atmospheric pressure to synthesize silver nanoparticles, *Int J Min Sci Technol*, 24 (2014) 251.
 - 19 Dong Z, Jiang T, Xu B, Yang J, Chen Y, Li Q & Yang Y, Comprehensive recoveries of selenium, copper, gold, silver and lead from a copper anode slime with a clean and economical hydrometallurgical process, *Chem Eng J*, 393 (2020) 124762.
 - 20 Palden T, MacHiels L, Onghena B, Regadio M & Binnemans K, Selective leaching of lead from lead smelter residues using EDTA, *RSC Adv*, 10 (2020) 42147.
 - 21 Gargul K, Boryczko B, Bukowska A, Jarosz P & Małeckı S, Leaching of lead and copper from flash smelting slag by citric acid, *Arch Civ Mech Eng*, 19 (2019) 648.
 - 22 Halim C E, Scott J A, Natawardaya H, Amal R, Beydoun D & Low G, Comparison between acetic acid and landfill leachates for the leaching of Pb(II), Cd(II), As(V), and Cr(VI) from cementitious wastes, *Environ Sci Technol*, 38 (2004) 3977.
 - 23 Davenport J R & Peryea F J, Phosphate fertilizers influence leaching of lead and arsenic in a soil contaminated with lead arsenate, *Water Air Soil Pollut*, 57 (1991) 101.
 - 24 Wang L, Mu W N, Shen H T, Liu S M & Zhai Y C, Leaching of lead from zinc leach residue in acidic calcium chloride aqueous solution, *Int J Miner Metall Mater*, 22 (2015) 460.
 - 25 Gil-Díaz M, Ortiz L T, Costa G, Alonso J, Rodríguez-Membibre M L, Sánchez-Fortún S, Pérez-Sanz A, Martín M & Lobo M C, Immobilization and leaching of Pb and Zn in an acidic soil treated with zerovalent iron nanoparticles (NZVI): Physicochemical and toxicological analysis of leachates, *Water Air Soil Pollut*, 225 (2014) 1.
 - 26 Levenspiel O, Chemical reaction engineering (3rd Edition) Levenspiel Octave, (1999).
 - 27 Park J Y & Levenspiel O, The crackling core model for the reaction of solid particles, *Chem Eng Sci*, 30 (1975) 1207.
 - 28 Prasannan P C, Ramachandran P A & Doraiswamy L K, A Model for gas-solid reactions with structural changes in the presence of inert solids, *Chem Eng Sci*, 40 (1985) 1251.
 - 29 Afshar E A, Ebrahim H A & Jamshidi E, Solving partial differential equations of gas-solid reactions by orthogonal collocation, *Comput Chem Eng*, 32 (2008) 1746.
 - 30 Dassori C G, Tierney J W & Shah Y T, Transient analysis of the particle-pellet model with structural changes in the solid phase, *Sadhana*, 10 (1987) 115.
 - 31 Janowski J, Barański A, Łagan M, Nedoma J & Sadowski A, On the application of the crackling core model to the reduction of magnetite to wustite, *React Sol J*, 8 (1990) 103.
 - 32 Ramachandran P A & Smith J M, Effect of sintering and porosity changes on rates of gas-solid reactions, *Chem Eng J*, 14 (1977) 137.
 - 33 Wen C Y, Noncatalytic Heterogeneous solid-fluid reaction models, *Ind Eng Chem*, 60 (1968) 34.
 - 34 Ramachandran P A & Smith J M, A single-pore model for gas-solid noncatalytic reactions, *AIChE J*, 23 (1977) 353.
 - 35 Wakao N & Smith J M, Diffusion in catalyst pellets, *Chem Eng Sci*, 17 (1962) 825.